

## Leading role of internal dynamics in the 2009 Indian summer monsoon drought

J. M. Neena,<sup>1</sup> E. Suhas,<sup>1</sup> and B. N. Goswami<sup>1</sup>

Received 15 November 2010; revised 6 March 2011; accepted 6 April 2011; published 7 July 2011.

[1] Understanding the underlying dynamics of the Indian summer monsoon (ISM) extremes such as severe droughts is key to improving seasonal prediction of the ISM rainfall. A large number of ISM droughts over the past century occurred unrelated to external forcing like the El Niño–Southern Oscillation (ENSO). In this study, we challenge the perception that the 2009 ISM drought was driven by ENSO and show that it was caused by internally driven processes. The 2009 drought of ISM was the result of two very long breaks, one in the month of June and the other in July–August (JA). While some studies provide strong evidence that the June break was caused by dry air intrusion associated with extratropical waves, a mechanism for the equally important JA break has not been elucidated so far. In this study, we unravel a new process in which westward propagating convectively coupled planetary-scale equatorial Rossby (PSER) waves emanating from the eastern Pacific as a remnant of Madden-Julian Oscillation (MJO), interact with the monsoon intraseasonal oscillation (MISO), modulate the active/break spells, and thereby influence the seasonal mean. It was found that during JA 2009 the arrival of the divergent phase of this PSER mode over the ISM domain reinforced and extended the break condition initiated by the northward propagating MISO, thereby creating a long break. Nonlinear kinetic energy exchanges between the PSER mode and the northward propagating MISO were found to be at the heart of such interactions. Evidence of such interactions can be seen during different active/break events in other monsoon seasons as well. As both long breaks were primarily driven by internal dynamical processes of the atmosphere, the study underscores the major role played by internal dynamics in causing the 2009 ISM drought. Our discovery that interactions between PSER waves and MISO can lead to significant modulations of the active/break spells opens up a new unexplored mechanism for understanding monsoon variability.

**Citation:** Neena, J. M., E. Suhas, and B. N. Goswami (2011), Leading role of internal dynamics in the 2009 Indian summer monsoon drought, *J. Geophys. Res.*, 116, D13103, doi:10.1029/2010JD015328.

### 1. Introduction

[2] The Indian summer monsoon (ISM) of the year 2009 was one of the worst failures over the last 100 years. The whole country suffered from the effects of a severe drought which lead to immense agricultural loss and affected the life and living of millions of people. The seasonal mean (June to September, JJAS) rainfall recorded a deficit of 22% of its long-term mean. The seasonal mean rainfall is largely determined by the intraseasonal monsoon activity manifesting as active and break conditions in rainfall [Goswami *et al.*, 2006; Goswami and Xavier, 2005a]. The active and break spells of monsoon are manifestations of monsoon intraseasonal oscillation (MISO) with preferred time scales between 10 and 20 days and 30 and 60 days [Sikka and Gadgil, 1980; Webster, 1987] (consult Goswami [2005a]

for a review). Due to the fact that the spatial structure of MISO has significant projection on that of interannual variation of the seasonal mean, frequency of occurrence of active/break spells can influence the seasonal mean. For example during certain years, the monsoon season may witness longer duration break spells and shorter active spells and lead to a drought condition. Most ISM drought years are associated with long breaks [Joseph *et al.*, 2009] and the drought of 2009 was not an exception, being the result of two prolonged breaks during the JJAS season (Figure 1a). The first break covering almost the month of June caused the June mean rainfall to be 47% below normal, the July–August (JA) break which extended from end of July to second week of August resulted in a deficit of 27% in August mean rainfall and the September mean rainfall also fell short by 21%. The brief active spells during July (with July recording near normal (98%) rainfall) and late August were not sufficient to overcome the rainfall deficit caused by these long breaks. The failure of the global models in forecasting the severe drought of 2009 monsoon,

<sup>1</sup>Indian Institute of Tropical Meteorology, Pune, India.

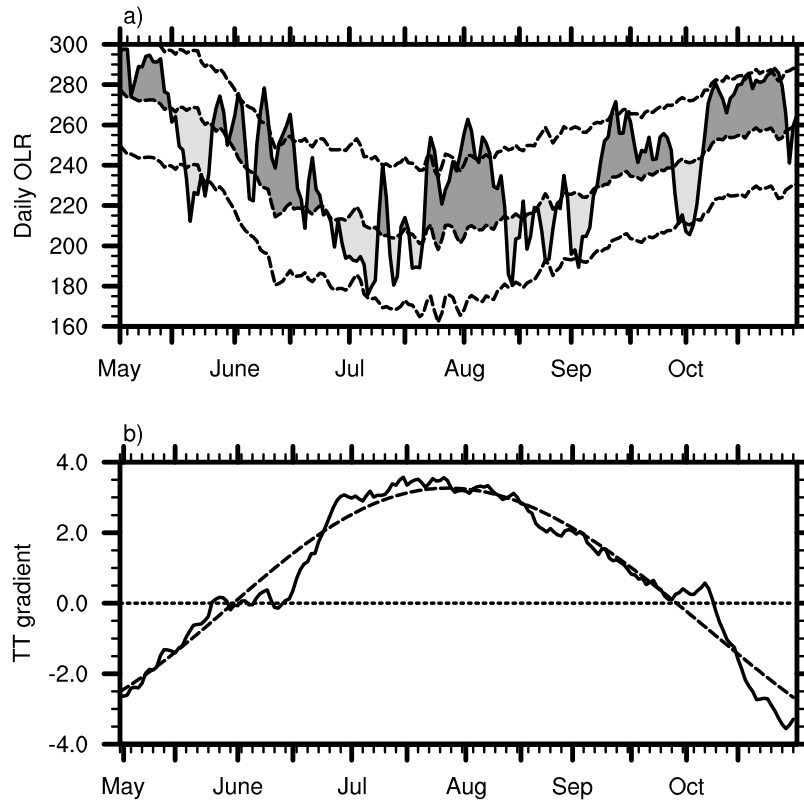


**Figure 1.** (a) Daily mean OLR ( $\text{W/m}^2$ ) averaged over the central India ( $15^\circ\text{N}$ – $27.5^\circ\text{N}$ ,  $70^\circ\text{E}$ – $85^\circ\text{E}$ ) during 1 May to 31 October 2009. Active (deviations below daily climatology) and break (deviations above daily climatology) phases are shown by light and dark shading, respectively. The daily  $\pm 0.5$  standard deviations of OLR are shown by the dashed lines. (b) Daily mean meridional tropospheric temperature (TT) gradient (solid curve,  $^\circ\text{K}$ ) estimated by taking the difference of vertically averaged (700–200 hPa) TT over the north box ( $30^\circ\text{E}$ – $110^\circ\text{E}$ ,  $10^\circ\text{N}$ – $35^\circ\text{N}$ ) and that over the south box ( $30^\circ\text{E}$ – $110^\circ\text{E}$ ,  $15^\circ\text{S}$ – $10^\circ\text{N}$ ) for the period 1 May 2009 to 31 October 2009. Dashed curve represents daily climatology of the TT gradient.

has invoked several investigations to understand the causative factors responsible for 2009 drought. Since the global monsoons are systems of high complexity governed by several processes of atmospheric and oceanic origin, diagnostic analysis of such extreme monsoon behavior provides an opportunity for understanding and predicting the monsoons in a better way.

[3] Active/break phases in monsoon rainfall are largely “internally” driven processes (of atmospheric origin) caused by the monsoon intraseasonal oscillations (MISOs) [Hoyos and Webster, 2007; Goswami, 2005a]. However, large scale “external” forcing (changes in boundary condition) such as the El Niño–Southern Oscillation (ENSO) may also play a role in determining the strength and duration of the active/break spells. ENSO can modulate the monsoon seasonal cycle in such a way that the season is dominated by larger/longer break spells and weaker/shorter active spells. Hence El Niño conditions over east Pacific are often accompanied by ISM droughts. The cooccurrence of El Niño and the ISM drought in 2009, gave rise to a general perception that the drought was externally driven by the El Niño forcing. Modeling studies by Ratnam *et al.* [2010] also arrived at a similar conclusion for the drought of 2009. However, it would be unwise to attribute the behavior of a complex monsoon system

to any one factor, especially when the linear correlation between ENSO and monsoon in recent decades is weakening [Kumar *et al.*, 1999; Goswami, 2005b]. The large biases of models in simulating the seasonal mean monsoon and inadequacies in model experiments does not permit to draw definitive conclusions from these model results. Hence the notion of 2009 drought being externally driven remains inconclusive and in this study we explore the relative role played by internal dynamics in causing the drought.

[4] Rather compelling evidence has been presented to show that the long break in June 2009 was internally driven by midlatitude waves [Krishnamurti *et al.*, 2010; Sikka *et al.*, 2010]. Krishnamurti *et al.* [2010] considered the major break condition in June to be instrumental in causing the 2009 ISM drought and explored possible mechanisms which lead to this extended break. They showed that dry desert air incursion associated with a blocking high over Arabian Peninsula retarded the growth of deep convection over central India and reduced the rainfall in June. However, the mechanism which caused the equally important JA break has not been suitably explored. Even though the August deficit is only 27% while that of June is 47%, it may be noted that the August mean rainfall is much larger than that of June rainfall particularly over central India and a

deficit of 27% makes a significant contribution to the seasonal mean rainfall. Hence, in this study we try to elucidate the physical mechanism which produced the long break in JA 2009. The highlight of this study is the finding that, besides having a direct effect on the MISOs, MJO can also exert a remote influence on ISM through planetary scale equatorial Rossby (PSER) waves and this mechanism was instrumental in causing the long break in JA 2009. Even though the dominance and role of PSER waves is very distinct in 2009, this is not an isolated case. As we show in the study, PSER waves have often been instrumental in modulating the MISOs in the past as well. Thus a new process is unraveled in this study with significant potential influence not only on the predictability of MISO but also on the variability of the seasonal mean monsoon. The article is structured in the following way. In section 2 the data and methodology are presented. In section 3 the results are presented, Large scale influence of El Niño on ISM are examined in section 3.1, the midlatitude westerly wave incursions and its implications are discussed in 3.2, the role of BISOs and the direct and remote influences of the MJO are presented in section 3.3 and 3.4 respectively. Finally, the summary and conclusions are given in section 4.

## 2. Data and Methodology

[5] The primary data sets used for the present study are interpolated Outgoing Long Wave radiation (OLR) from NOAA and zonal and meridional winds at 850 hPa and 200 hPa, temperature and humidity at all available levels from NCEP-NCAR reanalysis [Kalnay et al., 1996] for the year 2009. The real time multivariate MJO (RMM) indices constructed by Wheeler and Hendon [2004] obtained from <http://cawr.gov.au/staff/mwheeler/maproom/RMM/>. Anomaly fields were calculated by removing climatology from the daily data. The annual cycle of different parameters were computed by retaining the annual mean and first three harmonics. Lanczos filter [Duchon, 1979] was applied to the daily fields from 1 January 2009 to 31 December 2009 to bring out the 30–90 day (121 filter weights) and 15–30 day (141 filter weights) modes. It is verified that the results are independent of length of the time series and number of filter weights. The space-time variability of 15–30 day,  $-4$  to  $-2$  zonal wave number mode was extracted by applying Fourier based wave number–frequency filter [Wheeler and Kiladis, 1999]. Equatorial wave modes including MJO were separated by applying complex fast Fourier transform (FFT) in space and time for the June–September (JJAS) period and the resultant raw power spectra was normalized with the empirically estimated red background (consult Wheeler and Kiladis [1999] for more details). Singular Spectral Analysis (SSA) is carried out to bring out the dominant time scales of ER activity over the ISM domain [Ghil et al., 2002].

## 3. Results

### 3.1. Large-Scale El Niño–ISM Teleconnection

[6] A large scale forcing that can modulate the monsoon annual cycle and affect seasonal mean monsoon rainfall, is the ENSO. The ENSO-monsoon teleconnection can occur through a number of atmospheric pathways. El Niño can

affect monsoon through tropical teleconnection via modulating the equatorial Walker circulation and also through extratropical teleconnection by generating stationary Rossby waves in midlatitude westerlies through Rossby wave dispersion from tropics to midlatitudes [Hoskins and Wang, 2005]. Incursion of these midlatitude Rossby waves into the tropical domain may lead to cold air incursion and weaken the tropospheric temperature (TT) gradient which drives the monsoon circulation [Goswami and Xavier, 2005b]. Better known is the mechanism in which the SST anomalies over eastern Pacific modulates the equatorial Walker circulation such that convection becomes active over equatorial eastern Pacific and Indian Ocean, which in turn weaken the monsoon Hadley circulation and inhibit convection over the monsoon trough [Goswami, 2005b; Krishnamurthy and Goswami, 2000].

[7] During 2009 there was basin wide warming over equatorial and north Pacific [Ratnam et al., 2010], but the SST anomalies were not as large to consider it a strong El Niño case. In addition, the El Niño developed to its peak phase after the monsoon season. Also, as noted by Krishnamurti et al. [2010], the location of descending lobe of divergent circulation associated with ENSO (which determines regions of subsidence) did not fall over the ISM domain. Hence the notion of ENSO playing the major role in causing the ISM drought in 2009 is not well established. As any slowly varying forcing, ENSO is expected to influence a seasonal phenomenon like the ISM, primarily through modulation of the annual cycle. Through either mode of teleconnection, the influence of El Niño should be evident in the annual cycle and strength of monsoon circulation. As one of the pathways through which El Niño influences ISM is the TT gradient [Goswami and Xavier, 2005b; Xavier et al., 2007], we examine the annual cycle of TT gradient during 2009 and compare it with climatological TT gradient (Figure 1b). It is observed that the annual cycle of TT gradient is close to the climatological annual cycle (Figure 1b). On subseasonal timescales the TT gradient was significantly reduced during June break, however during JA break, the reduction in TT gradient is not significant.

[8] Another pathway through which El Niño influences ISM is through modulation of the Walker circulation. KE index of monsoon based on KE averaged over Tropical Easterly Jet (TEJ) region ( $0$ – $20^{\circ}\text{N}$   $50^{\circ}\text{E}$ – $80^{\circ}\text{E}$  at 200 hPa) embodies variation of the Walker circulation over the region and indicates a much weaker annual cycle for the El Niño composite compared to climatological annual cycle (Figure 2a). However, annual cycle for the year 2009 does not show this signature of weakened monsoon circulation. The intraseasonal evolution of the index shows weaker wind strengths at upper level during June break. Remarkably, no notable decrease is observed in the upper level KE during the JA break.

[9] Well known monsoon circulation indices such as the Monsoon Hadley index (MHI) [Goswami et al., 1999] and horizontal wind shear index [Wang and Fan, 1999] were also examined, which also did not reflect any significant weakening of circulation associated with ENSO. The MHI shows the weakened strength of meridional wind shear during the long break in June while such weakening is not observed during JA break (Figure 2b). The Wang and Fan index (WF) captures the weakened low level circulation

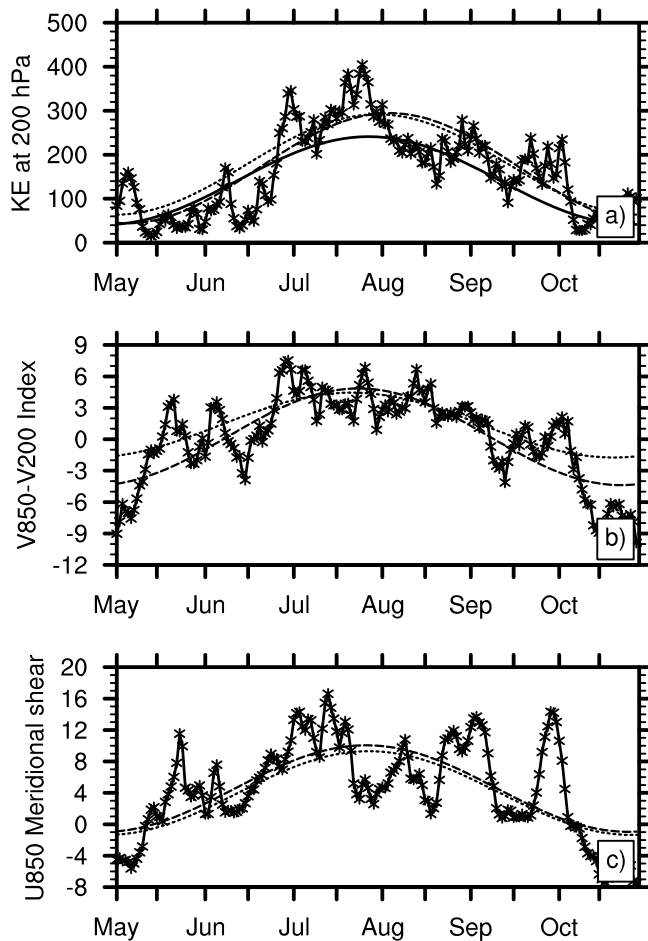


**Figure 2.** (a) Tropical easterly jet kinetic energy at 200 hPa averaged over the domain  $0^{\circ}$ – $15^{\circ}$ N,  $50^{\circ}$ – $80^{\circ}$ E (asterisks) along with the annual cycle for 2009 (dashed curve), climatological annual cycle (dotted curve), and the annual cycle composited over El Niño years (solid curve). (b) Monsoon Hadley circulation index; vertical shear of meridional wind (V850–V200) averaged over  $70^{\circ}$ E– $110^{\circ}$ E,  $10^{\circ}$ N– $30^{\circ}$ N (asterisks) along with its annual cycle (dashed curve) and the climatological annual cycle (dotted curve). (c) Indian summer monsoon index (U850 ( $5^{\circ}$ N– $15^{\circ}$ N,  $40^{\circ}$ E– $80^{\circ}$ E)–U850 ( $20^{\circ}$ N– $30^{\circ}$ N,  $70^{\circ}$ E– $90^{\circ}$ E)) (asterisks), along with its annual cycle (dashed curve) and the climatological annual cycle (dotted curve).

during JA break (Figure 2c). The above evidences, besides challenging the notion of an ENSO dominated drought, suggest that the two long breaks of 2009 may have been brought out by different mechanisms driven by internal dynamics of the atmosphere.

**3.2. Midlatitude Instabilities and Their Influence**

[10] It was shown by *Krishnamurti et al.* [2010] that desert air incursion from Arabian region had an important role in causing the long break in June 2009. The upper level circulation fields shows strong westerly wind anomalies at 200 hpa during June break (Figure 3a). A strong cyclonic circulation anomaly is seen over West Asia around  $60^{\circ}$ E,  $35^{\circ}$ N, and an anticyclonic vorticity is seen over east Asia at

$100^{\circ}$ E indicating the intrusion of midlatitude Rossby waves to as far as  $25^{\circ}$ N during June. The incursion of midlatitude disturbances are associated with cold air advection over central India which can affect the north-south temperature gradient, weaken the strength of monsoon circulation and lead to break conditions [*Ramaswamy, 1962*]. Internal interactions between the Rossby wave response to suppressed convection and midlatitude westerlies can also lead to prolonged breaks [*Krishnan et al., 2009*]. There is general consensus that the westerlies associated with midlatitude wave troughs and the Blocking High over southern Arabia advected cold dry air toward Indo-Pak and central Indian regions during June break and curbed the moisture influx to the ISM domain [*Krishnamurti et al., 2010; Sikka et al., 2010*].

[11] The 200 hPa circulation during the JA break is shown in Figure 3b. The midlatitude westerlies are found to the north of  $35^{\circ}$ N and no westerly wave incursion is observed in the ISM domain. It may be noted that the TT gradient is not as large as that during June break (Figure 1b). If the midlatitude Rossby waves were a stationary response to El Niño forcing, it would have persisted during JA also. Since it is not the case, it can be surmised that the midlatitude Rossby wave incursion was a transient atmospheric phenomenon not directly related to ENSO. These observations indicate that the JA break was not caused by midlatitude Rossby wave incursion.

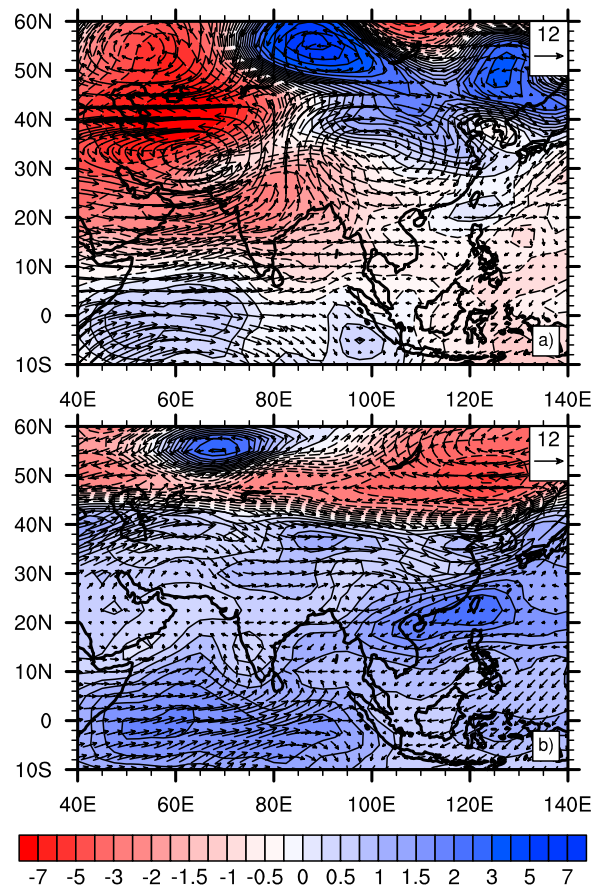


**Figure 3.** (a) Composite of temperature (shaded and contoured) and wind anomaly at 200 hPa during June break. (b) Same as Figure 3a but for July–August break.

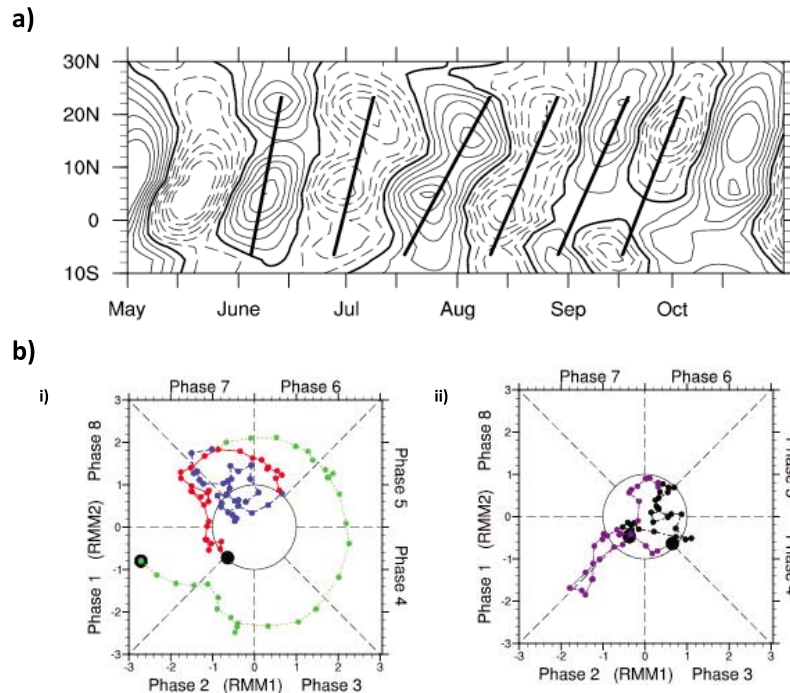


**Figure 4.** (a) Time-latitude Hovmöller diagram of 30–90 day band-pass filtered daily OLR anomaly ( $\text{W/m}^2$ ) averaged over  $70^\circ\text{E}$ – $85^\circ\text{E}$  for the period 1 May 2009 to 31 October. Solid contours represent positive anomaly, and dashed contours represent negative anomaly. Contours are drawn from  $-30$  to  $30$  with uniform interval  $6$ . (b) MJO life cycle in RMM1 and RMM2 phase space (left) during April (green), May (blue), and June (red) 2009 and (right) during July (purple) and August (black) 2009.

### 3.3. Boreal Summer ISOs

[12] The MISOs and eastward propagating equatorial MJO [Madden and Julian, 1972, 1994] constitute the boreal summer ISOs (BISOs). The dominant intraseasonal variability of tropical atmosphere, BISOs is also a determining factor behind the evolution of the ISM. Northward propagation of MISO is shown in the latitude time plot of 30–90 day filtered OLR anomalies averaged over ISM longitudes (Figure 4a). It captures the JA break from around 20 July to second week of August (Figure 4a). This indicates the dominance of MISO during the JA period. The midlatitude influences being weak during this period, we need to examine the other factors which may have had an influence on the MISO to cause this extended break.

[13] Even though the equatorial eastward propagating summer MJO convective anomalies are not as strong as its winter counterpart, it is intrinsically linked to the northward propagating MISOs [Wang and Xie, 1997; Kemball-Cook and Wang, 2001]. The MJO is a planetary scale (wave number 1–3, 30–90 day period) phenomenon that modulates not only weather and synoptic scales but also the seasonal mean Asian and Australian monsoon [Maloney and Hartmann, 2001; Bessafi and Wheeler, 2006; Pai et al., 2009; Wheeler et al., 2009]. The linkage between the different phases of MJO life cycle and MISO was examined by Pai et al. [2009]. It was noted that about 83% of the ISM breaks occurred when the MJO active phase was over the eastern Pacific, Atlantic and western Indian Ocean. Although the results were statistically robust, no physical argument was provided to support this observation.

[14] During premonsoon period of 2009 the MJO activity was significantly high (Figure 4b). The life cycle of MJO during premonsoon and monsoon season (1 April 2009 to 31 August 2009) was analyzed using the RMM indices formulated by Wheeler and Hendon [2004]. The indices are constructed from combined empirical orthogonal function (CEOF) analysis of 850 hPa zonal wind, 200 hPa zonal wind and OLR. Although the RMM indices may have contributions from convectively coupled Kelvin waves, ER waves and inertia-gravity waves [Roundy et al., 2009],

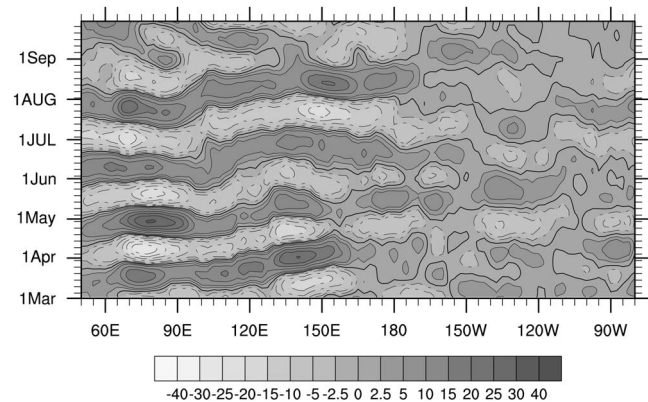


**Figure 5.** Time-longitude Hovmöller diagram of 30–90 day band-pass filtered daily OLR anomaly averaged over  $10^\circ\text{S}$ – $10^\circ\text{N}$  latitudinal domain for the period 1 March 2009 to 30 September 2009.

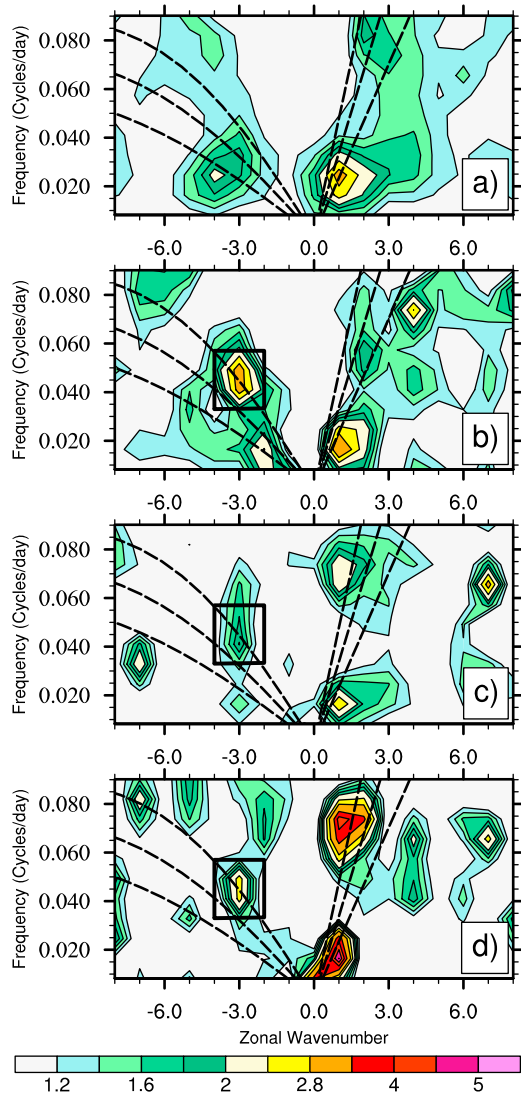


**Figure 6.** (a) Symmetric raw/background wave number–frequency spectra of OLR for 15 summer seasons (JJAS, 1994–2008), power greater than 1.2 is statistically significant at 95% confidence level. Symmetric raw/background wave number–frequency spectra for summer (JJAS) of 2009 of (b) OLR, (c) zonal wind at 850 hPa, and (d) zonal wind at 200 hPa. Power greater than 2.3 is statistically significant at 95% confidence level. The power in ER (wave number  $-4$  to  $-2$ , period 15–30 days) is highlighted in the square boxes. Dispersion curves are shown by dashed curves.

the projection of daily data on combined multivariate pattern enhance the signal-to-noise ratio and capture large scale MJO fluctuations. The life cycle of summer MJO during 2009 in RMM1–RMM2 phase space is shown in Figure 4b. It is observed that MJO became active around last week of March and covered the distance between Atlantic and Pacific by the end of April. During May, MJO went into the weak phase; it rejuvenated again during the 1st week of June and traveled eastward from Pacific to Atlantic. It was active till 15 June and then it decayed and died. Though MJO was active during May and June, the active phase of MJO was over Pacific and Atlantic (phases 7 and 8) and hence it

rules out the possibility of MJO causing the early ISM onset. As additional evidence, eastward propagation of 30–90 day band-pass filtered daily OLR was examined for the period 1 March to 30 September 2009. Corroborating the inferences derived from RMM phase space, it is seen that MJO was strong during premonsoon period and propagated beyond the date line (Figure 5). Some eastward propagation is observed during monsoon season but its amplitude is rather weak and the propagation is not as clear as that during premonsoon time.

[15] The role of MJO in producing long breaks was examined by *Joseph et al.* [2009]. They argued that the MJO dry condition over eastern equatorial Indian Ocean and active condition over central Pacific produce westerly wind burst over the western equatorial Pacific that extend the warm pool to the east and sustain the active phase of MJO over the central Pacific for a longer time. As a result the divergent Rossby wave associated with this phase, propagating westward from western Pacific to the ISM domain also has a longer life. This may cause very long breaks and lead to a drought in ISM. The confinement of active MJO to the eastern hemisphere during June, reject the possibility that it may have directly caused the June break in 2009. As evident from the RMM phase space (Figure 4b), MJO activity was very weak during the JA months. Hence such direct influence of MJO may not have played a role in the JA break of 2009. The one possibility which remains to be examined is the delayed influence of MJO reaching the ISM domain during JA break.

### 3.4. Role of Remote Influence of MJO

[16] Examination of the phases of MJO and MISO, revealed that there is a statistical probability for MISO to go in to a convectively inactive state when the MJO is over phases 7 and 8 [*Pai et al.*, 2009]. During the June break of 2009 the MJO was active in phases 7 and 8 (Figure 4b). However, no clear physical link is known, which can explain how an event occurring over the eastern Pacific separated by such large distances, bring out a significant change over the ISM domain. In order for the MJO activity over the eastern Pacific to be the driving force for the concurrently occurring ISM break, there should be a fast westward propagating carrier of planetary scale unaffected by the strong mean flow. The known westward propagating mode in the equatorial region is the equatorial Rossby (ER) mode which, at a phase speed of about 5–6 m/s would take about 45–50 days to cross this distance. Though it rejects the part of MJO in producing June break, it opens up the possibility of exploring the role of MJO in producing the JA break.

[17] The wave number–frequency distribution of OLR power is used for quantifying the influence of equatorial wave modes in modulating the tropical convection [*Wheeler and Kiladis*, 1999; *Kiladis et al.*, 2009]. The space-time spectrum normalized by its own red background for 15 summer (JJAS) seasons (1994–2008) is shown in Figure 6a, overlapped with the dispersion curves corresponding to equatorial wave modes [*Matsuno*, 1966]. It shows statistically significant power at 95% confidence level (power greater than 1.2) in MJO, convectively coupled Kelvin waves and  $n = 1$  ER waves. The dominant quasi-biweekly mode of the western Pacific is not seen as a prominent mode probably due to power leakage across the wave numbers from Fourier

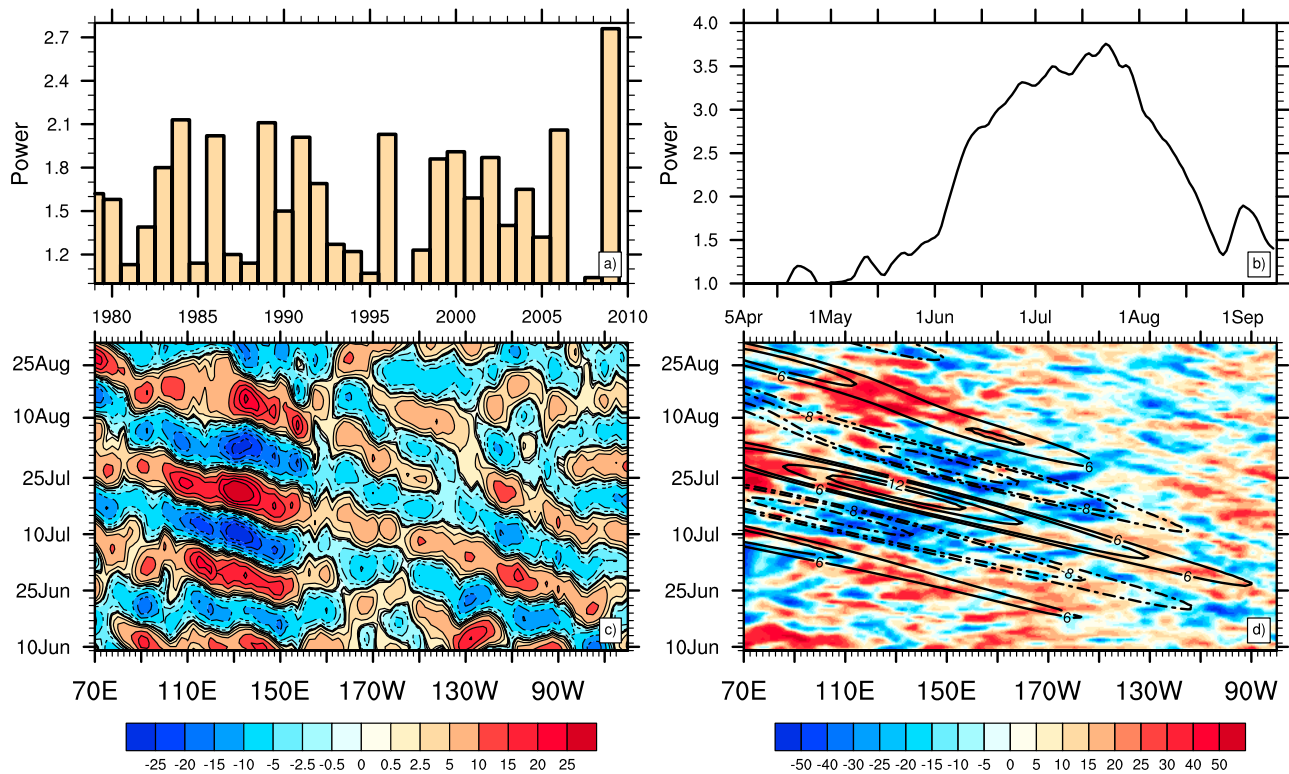


**Figure 7.** (a) Symmetric raw/background wave number–frequency power averaged over period 15–30 days and wave number -3 for the 1979–2009 JJAS seasons. (b) Symmetric raw/background wave number–frequency power calculated using sliding window of length 72 days, averaged over period 15–30 days and wave number -3. Dates given in abscissa correspond to center of the sliding window. (c) Longitude-time diagram of 15–30 day band-pass filtered OLR anomalies averaged over 0°–20°N during 10 June 2009 to 31 August 2009. (d) Same as Figure 7c but for total OLR anomalies (daily climatology removed, shaded) overlaid with the wave number–frequency (-4 to -2 and 15–30 day period) filtered OLR anomalies (contours; solid contours represent positive anomalies).

decomposition in space. Often the space time distribution of ER modes is washed out by interaction with the strong background flows [Kiladis *et al.*, 2009]. Hence, the most notable feature is the significant power in ER, centered on wave number -4 in the 30–50 day period. But the power is as not as strong as that of the MJO. Whereas, the JJAS spectra for 2009 shows the ER mode to be as strong as the MJO and maximum power is centered on planetary scale -3 at a shorter periodicity of 15–30 days (Figure 6b). To verify whether the observed ER mode is convectively coupled, the symmetric raw/background spectra of lower and upper level zonal winds were also examined (Figures 6c and 6d). They also exhibit power in the same wave number-frequency region as the ER mode in OLR spectra. A more robust and statistically significant power is observed in zonal wind at 200 hPa. Since OLR is best suited to extract the equatorial wave modes and as observed it clearly captures the ER mode, we have mainly used OLR in further analysis of ER mode (unless mentioned otherwise).

[18] In order to evaluate the existence of PSER mode in the 15–30 day time scale, the symmetric raw/background space-time power was averaged over the 15–30 day period at wave number -3 for the individual JJAS seasons from 1979 to 2009 (Figure 7a). The 95% significant level for the average power is 2.3. The year of 2009 seem to be unique,

as the ER wave with a periodicity of 15–30 days and wave number -3, has power much above the average power of all the years (Figure 7a). This raises an important question about what might have triggered the modulation of ER modes in wave number and frequency. Does this planetary scale convectively coupled ER mode have any link in producing the long break during JA?

[19] It is widely known that analysis based on Fourier decomposition has the drawback of suppressing time information. Even though 2009 JJAS space-time spectrum shows considerable power on ER wave modes, it is not apparent when the ER activity was prominent during the season. In order to identify the time of occurrence of peak ER activity during 2009 monsoon season, a symmetric raw/background wave number–frequency spectra of OLR was computed in a sliding window of length 72 days starting from 1 March. The average power over the 15–30 day period at wave number -3 is identified as the ER wave mode in each window. In Figure 7b the ER wave mode power corresponding to 5 April is the resultant of analysis for the 1 March to 11 May period, that for 6 April is the resultant of analysis for the 2 March to 12 May period and so on. The peak ER activity was found around 20 July. It corresponds to the window 16 June to 27 August. From this analysis it can be inferred that the significant ER activity

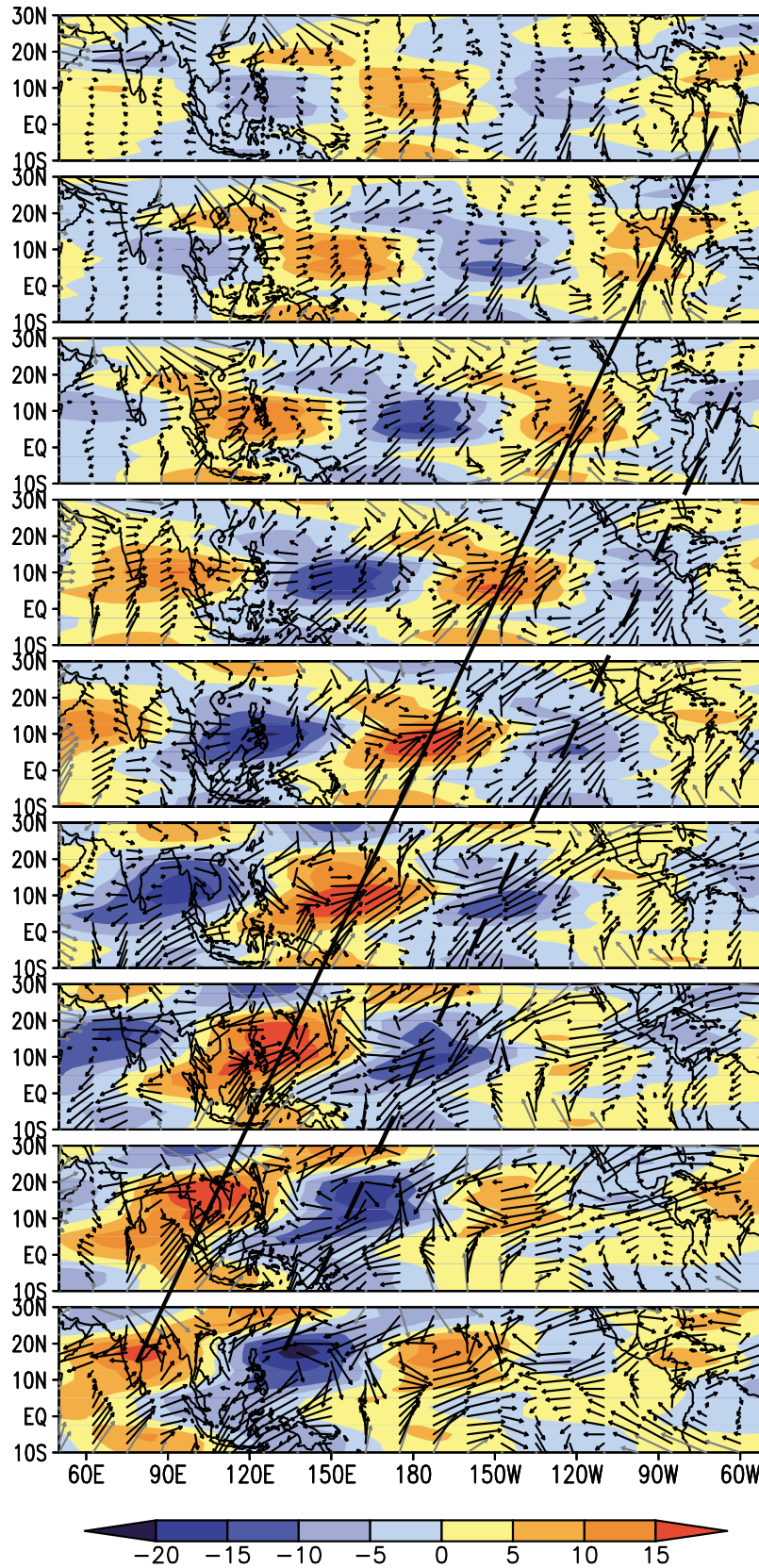


**Figure 8.** Five day averages of space-time filtered (15–30 days, wave numbers –4 to –2) OLR ( $W/m^2$ ) and wind (m/s) anomalies at 200 hPa, from (top to bottom) 21 June 2009, 26 June 2009, 1 July 2009, 6 July 2009, 11 July 2009, 16 July 2009, 21 July 2009, 26 July 2009, and 31 July 2009. Westward propagation of active (suppressed) convection is shown by solid (dotted) line.

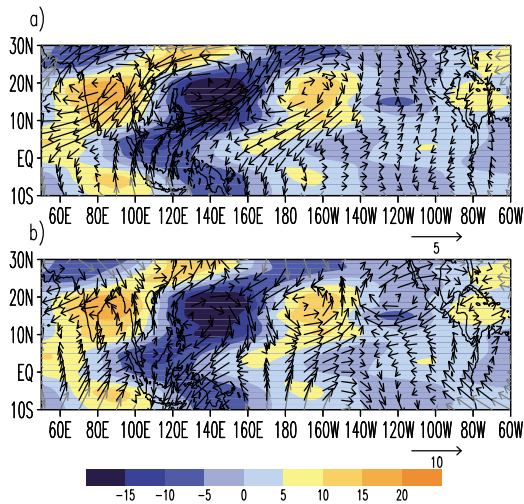


**Figure 9.** Spatial structure of ER waves on 1 August 2009 at (a) 850 hPa and (b) 200 hPa. ER waves are represented by 15–30 days, wave numbers  $-4$  to  $-2$  filtered anomalies of OLR (shaded) and wind (vectors).

occurred only during June–August period. These results are independent of the choice of window length. Does this PSER mode active during June to August period have any relationship with the MJO activity during early monsoon period?

[20] The Kelvin-Rossby couplet of MJO is the main planetary scale phenomenon active over the central equatorial Pacific during March to June period which could have an influence on the equatorial wave modes. The MJO travels as a Kelvin-Rossby couplet over the warm waters of the western Pacific and beyond the dateline it decays or decouples and is observed as an eastward propagating dry Kelvin wave [Hendon and Salby, 1994; Masunaga, 2007]. Although not conclusively established, such a decoupling can give rise to westward propagating Rossby modes [Hayashi and Sumi, 1986; Wang and Xie, 1997]. In an alternative viewpoint, Roundy and Frank [2004] proposed that eastward propagating ISO of large amplitude has the potential to trigger westward propagating ER modes either through modulation of convective anomalies or through interaction with north-south oriented mountain ranges on the west coast of America. The preferable spatial and temporal scales of such ER waves may also be altered through interaction with the eastward propagating ISOs. In the 2009 scenario, the developing phase of El Niño during premonsoon season provided the suitable environment for extending MJO convective activity farther eastward and sustaining it for quite a long time. From the RMM1–RMM2 phase diagram (Figure 4b) it can be inferred that the MJO started its decay phase around mid June over the eastern Pacific. To account for the presence of PSER modes in the Pacific region during June to August period, it may be hypothesized that the Rossby-Kelvin couplet of MJO may have decoupled into Rossby and Kelvin wave over the eastern Pacific and this decoupled Rossby wave might have been instrumental in modulating the ER mode in spatial and temporal scale. A possible wave reflection mechanism proposed by Roundy and Frank [2004] cannot also be dismissed. Even though a mechanism for generation and modulation of ER modes

cannot be established unambiguously from the observational analysis, the evidences imply that the PSER mode in the Pacific region during June to August period is most likely to be linked to the MJO.

[21] To bring out the role of PSER mode in producing the long breaks in 2009, the ER wave is extracted by applying 15–30 day band-pass filter in time. It is clear from the wave number frequency diagram that only the ER mode shows statistically robust signal in this time scale, hence the resultant time series can be considered as representative of the ER wave. The longitude-time diagram of 15–30 day filtered OLR shows continuous westward propagation starting from central and eastern Pacific (Figure 7c). The anomalies strengthen in amplitude over the convectively active region of Western Pacific warm pool and further move westward to the ISM domain. Since convection over the ISM domain is also under the influence of this westward propagating mode along with the MISOs, a comparison of the phases of convection associated with the northward propagating 30–90 day MISO (Figure 4a) and that of the westward propagating PSER mode (Figure 7c) is necessary to understand the active/break phases. During the period of June break, the MISO over the ISM domain was detrimental for convection from 1 to 15 June followed by the convective phase around 23 June. The ER mode does not exhibit a planetary scale during this period and the westward propagating convective signal was observed to originate from west of the date line (Figures 7b and 7c). This provides further evidence to rule out the role of PSER mode during the June break.

[22] Large amplitude of time filtered OLR in Figure 7c indicate a robust westward propagating signal. Is this signal related to the PSER mode and is its presence evident in unfiltered OLR anomalies? To answer this question the time-longitude plot of total OLR anomalies averaged over  $0^{\circ}$ – $20^{\circ}$ N is shown in Figure 7d together with space-time filtered PSER wave anomalies ( $-4$  to  $-2$  wave numbers and 15–30 days). It is clear that the westward propagation of PSER signal can be seen even in the unfiltered OLR anomalies and that almost all of time filtered anomalies came from the ER waves.

[23] In order to further validate the robustness of the PSER waves, we examined the convectively coupled nature of the waves. For this purpose, the  $-4$  to  $-2$  wave number 15–30 day ER mode was extracted by space-time filtering of OLR and upper level winds. Pentad anomalies of space-time filtered ER mode are used to depict its large scale spatial structure and time evolution (Figure 8). The convectively coupled nature of ER mode is observed in the coherent westward propagation of circulation vortices and convection. The subsidence phase of the ER mode propagate westward from east Pacific in the first pentad (21 June 2009) and reaches the ISM domain ( $10^{\circ}$ – $20^{\circ}$ N,  $70^{\circ}$ – $80^{\circ}$ E) in the ninth pentad (1 August 2009), in a period of 45 days. The vertical structure and convective coupling of the ER mode is clearly depicted in Figure 9 by the OLR and, upper and lower level wind anomalies (shown for 1 August 2009). The ER mode exhibits a first baroclinic structure with two convective centers, one centered around  $16^{\circ}$ N and other around  $5^{\circ}$ S.

[24] During the JA break, the break phase of MISO dominated over the ISM domain. This break phase occurring by the end of July is one aspect of the climatologically

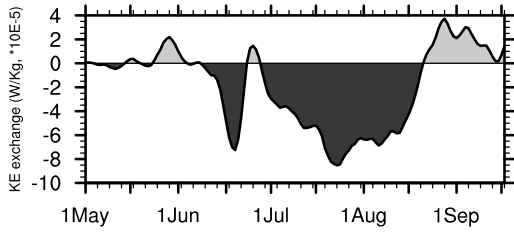


**Figure 10.** Rate of KE exchange per unit mass (W/kg) between 15 and 30 day and 60 day scale calculated at 850 hPa pressure level over the ISM domain (70°E–82.5°E, 12.5°N–25°N) using 60 day sliding window. Negative values indicate the flow of KE from 15 to 30 day to 60 day scale. The abscissa represents the middle date corresponding to each sliding window.

phase locked component of the ISO [Suhas and Goswami, 2008]. However, the question which remains is the cause for the amplification and longevity of this break phase. Examination of the ER mode shows that the first convective pulse of the PSER mode originates at 90°W around 15 June (note that it coincides with the decay phase of the MJO) and propagates westward with a phase speed of 6 m/s. It shows strengthening over the western Pacific and arrives over the ISM domain by 20 July, coinciding with the convective phase of MISO. The next pulse of positive OLR anomalies of the PSER mode originating from around 75°W on 20 June also show similar propagation characteristics, reach the ISM domain around end of July and superimpose on the existing break phase of the MISO. These subsidence anomalies have a periodicity of 15–30 day and they reinforced the

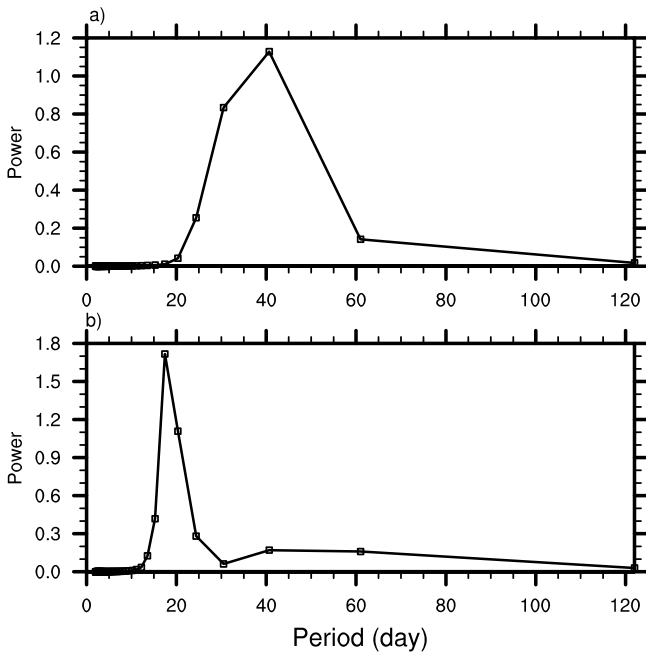


**Figure 11.** Power spectra of ER time series (1979–2009 JJAS) averaged over the ISM domain (10°N–25°N, 70°E–85°E) reconstructed from (a) first two modes of SSA and (b) third and fourth modes of SSA.

break phase of the MISO during the first week of August and caused the break phase to persist until 13 August.

[25] The large scale 30–60 day and 10–20 day modes account for a major part of the monsoon intraseasonal variability (ISV). Even though it is understood that active/break conditions in monsoon rainfall arise due to the combined effect of these two modes, the underlying interaction between these modes has not been elucidated so far. Estimation of nonlinear kinetic energy exchange in frequency domain is one possible method to bring out the interaction between these two modes over a region (consult Hayashi [1980] and Neena and Goswami [2010] for detailed methodology). Likewise here we examine the interaction between the high frequency (15–30 day) and the low frequency (30–60 day) modes of MISOs over the ISM domain. Since we are interested in bringing out the time evolution of such

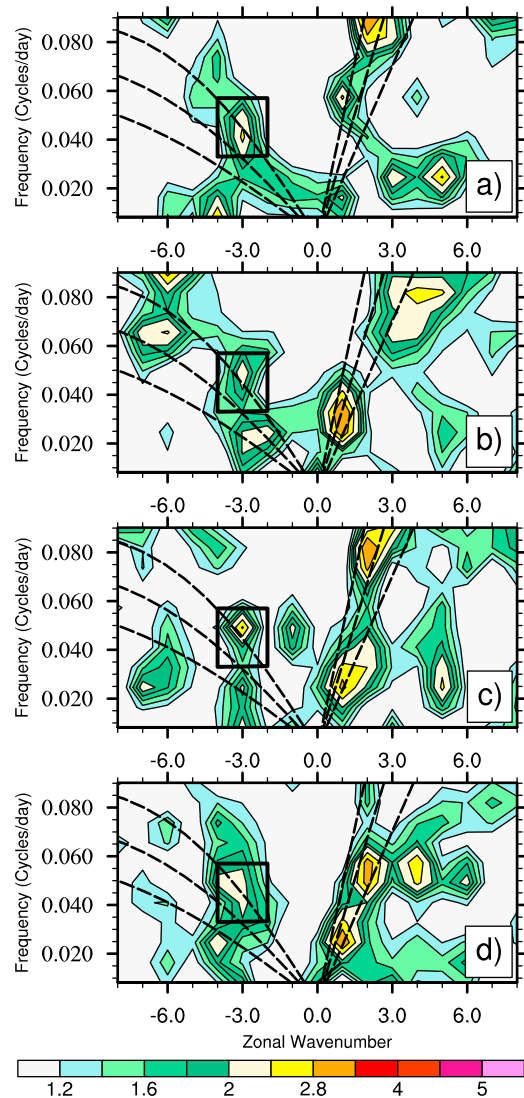


**Figure 12.** Symmetric Raw/Background wave number–frequency spectra of OLR for four summer seasons (JJAS): (a) 1984, (b) 1986, (c) 1989, and (d) 2006. The power in ER (wave number –4 to –2, period 15–30 days for the years 1984, 1986, 1989, and 2006) are highlighted in the square boxes. Dispersion curves are shown by dashed curves.

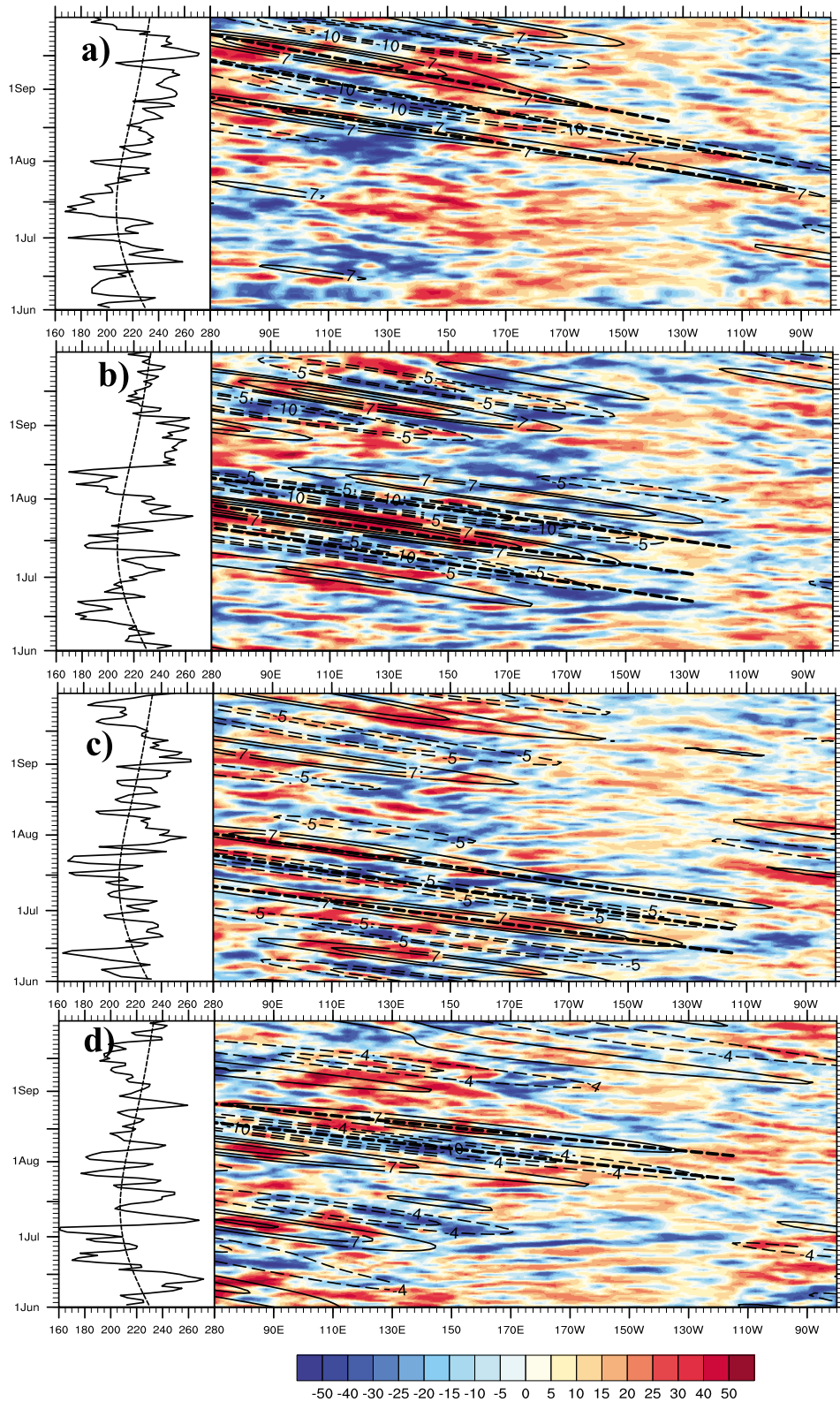


**Figure 13.** Arrival of the westward propagating ER modes compared with the active/beak phases over the ISM domain (5°N–20°N, 70°E–85°E) during the four summer seasons: (a) 1984, (b) 1986, (c) 1989, and (d) 2006. (left) Daily mean OLR (W/m<sup>2</sup>) averaged over the ISM domain along with the climatological annual cycle (dashed curve). (right) Longitude-time diagram of total anomaly (daily climatology removed) and space-time filtered OLR anomaly (contours, wave number –4 to –2 and period 15–30 day) averaged over 0°–20°N latitudes. Negative anomalies are shown by thin dashed contours. Thick dashed curves show the westward propagation of PSER wave.

interactions, we have to resort to the use of a sliding window. The length of the sliding window was appropriately chosen such that it can resolve the ISO scales and yet preserve the time information. The exchange was computed from 1 April to 17 October 2009 using a 60 day sliding window. KE exchange between 15 and 30 day (2–4 harmonics) and 60 day (1 harmonic) scale computed in each 60 day window is shown in Figure 10 against the middle date of each window. Although the use of only one harmonic in resolving the low frequency ISO scale may be treated as a caveat in the above analysis, it still gives useful information on the interaction during JA break. It is found that at the time of arrival of the PSER mode over the ISM domain, 15–30 day scale gives energy to the longer scale. Hence it can be inferred that there was strong interaction between the PSER mode and the MISOs over the ISM domain during the JA break indicating that both linear super position as well as nonlinear interactions played a significant role in amplifying and extending the JA break.

[26] Based on the above evidences we propose a mechanism in which the developing El Niño phase over the eastern Pacific helped sustain MJO convection and helped maintain the Kelvin Rossby couplet of MJO further eastward of date line. By mid June the MJO was in its decay phase and decoupled into a westward propagating Rossby wave and an eastward propagating dry Kelvin wave. The decoupled Rossby wave gave rise to the convectively coupled PSER mode in the 15–30 day time scale, which propagated westward from the eastern Pacific at a speed of about 6 m/s, gaining energy over western Pacific and reaching the ISM domain around end of July. It was the timing of the arrival of this mode with respect to that of the northward propagating MISO that was instrumental in causing the long break in JA 2009. The subsidence phase of the ER mode arriving over the ISM domain was during the peak break phase of MISOs. The linear super position as well as nonlinear interactions of these two modes further strengthened the break phase and prevented the development of convective activity over a longer period.

[27] The question which naturally arises is whether this mechanism is unique to 2009 or is it an overlooked aspect which might have modulated the active/break spells in the past? It is known that the ER mode encompass broad spatial and temporal scales [Wheeler and Kiladis, 1999; Kiladis et al., 2009]. Hence it is necessary to identify whether the PSER mode as observed in 2009 is a dominant ER mode which influences the ISM. The OLR anomalies from 1979 to 2009 is filtered for the broad ER scale (wave number  $-10$  to  $-2$ , period 10 to 100 days) and averaged over the ISM domain for JJAS months. The resultant time series is considered as representative of the ER activity over the ISM domain and the dominant time scales of ER mode are separated by applying SSA analysis on this time series. Two dominant modes are identified; representing a 40 day time scale (first two modes of SSA explaining about 35% of total variability) and a 20 day time scale (3rd and 4th modes of SSA explaining about 25% of total variability) respectively (Figure 11). The 20 day mode resembles the identified PSER mode. The years of significant PSER activity were isolated as when the raw/background power in PSER mode (wave number  $-3$ , 15–30 day period) exceeded a threshold of 2 (90% confidence level) (Figure 7a). Besides 2009, years like 1984, 1986, 1989, 1991, 1996, and

2006 exhibited significant PSER activity. The space-time spectra of OLR computed for the JJAS period for the years 1984, 1986, 1989, 2006 are shown in Figure 12. The daily OLR anomalies (daily climatology removed) clearly show a westward propagation from the eastern Pacific to ISM domain during all the years. The propagation of the ER wave was clearly brought out using space time filtered OLR anomalies (wave number  $-4$  to  $-2$ , 15–30 day period). Steady planetary scale westward propagation is seen in all the years in both set of anomalies (Figure 13). However, such propagation is not seen throughout the monsoon season but is rather limited to two or three events. This implies a transient causative mechanism which determines the generation of these waves. As in 2009, the ER wave propagation from central and eastern Pacific in all the years coincide with the MJO phase being in the region. The arrival of ER waves over the ISM domain is contrasted with the active or break conditions over the region (Figure 13). Similar to 2009 scenario, mostly the arrival of convective phase of the ER wave coincides with active condition and the subsidence phase of ER mode is followed by break condition.

#### 4. Summary and Conclusion

[28] The Indian subcontinent experienced a major drought in the year 2009, which resulted in immense agricultural and economic loss. The drought was a result of two long breaks which occurred during the peak monsoon season. Understanding the cause of these long breaks, therefore, is key to understanding the drought of 2009. Krishnamurti et al. [2010] had shown that the June break was internally driven by invasion of midlatitude wave troughs into the tropics. However, the equally important long break of JA has not yet been suitably explored. While close interaction of midlatitude instabilities with monsoon flow caused the extended break in June, the same reasoning does not hold for the JA break. In this study we unravel a new unexplored mechanism for causing the JA long break and attempt to comprehend the relative role of “internal” and “external” factors in causing the drought. Contrary to earlier perception, we show that the “external” influence of ENSO on the monsoon annual cycle was not dominant during 2009, indicating that internal dynamics had a decisive role in causing the drought.

[29] The strong equatorial convective activity in 30–90 day time scales was one of the notable features during 2009 premonsoon. The MJO activity in 2009 was extended further eastward to the eastern Pacific, favored by the developing El Niño. The RMM1-RMM2 phase diagram showed MJO activity to be strong over the Pacific and Atlantic in June. Since the active phase of MJO was over the eastern Pacific during the period, the possibility of influence on the ISM through westerly wind burst can be discarded. Also a physical mechanism through which the MJO convective activity over the eastern Pacific can simultaneously affect the ISM is not known. Therefore the possibility of MJO stimulated break in June does not hold ground. On the other hand we investigated the possible role of active MJO in June in producing the JA break of the ISM.

[30] The OLR space-time spectra for 15 summer seasons (JJAS) show the ER mode to be centered on wave number  $-4$  and at 30–50 day period (Figure 6a). However, a unique

feature observed in the wave number frequency spectra of OLR for JJAS 2009 is the existence of unusually large power in PSER (wave number  $-3$ , period 15–30 days) waves with peak activity during mid June to August period. This PSER mode exhibits a convectively coupled, first baroclinic vertical structure and are found to originate from the eastern Pacific. PSER modes in the eastern Pacific could either arise from interaction between eastward propagating ISO with topography or from modulation of convective anomalies by eastward propagating ISO [Roundy and Frank, 2004]. Decoupling of planetary scale MJO can also possibly give rise to westward propagating ER modes. The initiation of westward propagating ER mode in 2009 being coincident with the decay phase of MJO over the eastern Pacific suggests its possible relation to decoupling MJO.

[31] While the continuous westward propagating PSER mode is not evident during early June, an unbroken westward propagating signal starting from around  $75^{\circ}\text{W}$  on 20 June and reaching the ISM domain around 1st week of August is observed in total (unfiltered) OLR anomalies as well as in 15–30 day band-pass filtered OLR anomalies. Consistent and coherent westward propagation of convection and circulation vortices is also observed in the wave number–frequency filtered anomalies of OLR and winds. Spatiotemporal evolution of ER mode brought out by five day averages of space–time filtered anomalies, show that the subsidence phase of the ER mode initiated over the eastern Pacific in the first pentad (21 June), propagated westward and reached the ISM domain in the ninth pentad (1 August), in a period of 45 days. The ISM domain being dominated by the northward propagating MISO was in the break phase at the same time. Arrival of the subsidence phase of the ER mode by 1 August reinforced the break condition over the ISM domain and caused the strengthening and extension of break to around 13 August. Computation of nonlinear KE exchange between these two modes also confirmed strong interaction between the modes during the period. Putting together these evidences we conclude that, the MJO activity over the eastern Pacific gave rise to convectively coupled PSER waves which propagated westward toward the ISM domain and interacted with the MISO to strengthen and extend the suppressed phase of convection.

[32] Thus the study concludes that even in the ENSO forced environment of 2009 monsoon season, the internal instabilities of the atmosphere, which includes the tropical ISOs and the midlatitude instabilities, were responsible for the two long breaks in the ISM and caused one of the worst droughts in the past century. While the first long break in June was brought out by midlatitude wave incursion, the highlight of the present study is a new unexplored mechanism in which MJO activity in the eastern Pacific can remotely affect the ISO phase over the ISM domain through PSER waves. Further investigations revealed that the 15–30 day mode of ER wave is one of the dominant modes observed over the ISM domain and evidences confirming the role of PSER waves in modulating the active/break spells over the ISM domain were found during different monsoon seasons. Since the PSER activity was also prevalent during non–El Niño years, we infer that the mechanism may not be wholly dependent on an El Niño dominated background state. The mechanism presented in this study

adds a new complexity to the extended range prediction of active/break spells. However, the mechanism of decoupling of the MJO and the modulation of ER waves needs further investigation.

[33] **Acknowledgments.** N.J.M. and S.E. acknowledge CSIR for a fellowship. B.N.G. and I.I.T.M. are fully supported by Ministry of Earth Sciences, Government India, New Delhi.

## References

- Bessafi, M., and M. C. Wheeler (2006), Modulation of South Indian Ocean tropical cyclones by the Madden-Julian Oscillation and convectively coupled equatorial waves, *Mon. Weather Rev.*, *134*, 638–656, doi:10.1175/MWR3087.1.
- Duchon, C. E. (1979), Lanczos filtering in one and two dimensions, *J. Appl. Meteorol.*, *18*, 1016–1022, doi:10.1175/1520-0450(1979)018<1016:LFIOAT>2.0.CO;2.
- Ghil, M., et al. (2002), Advanced spectral methods for climatic time series, *Rev. Geophys.*, *40*(1), 1003, doi:10.1029/2000RG000092.
- Goswami, B. N. (2005a), South Asian monsoon, in *Intraseasonal Variability of the Atmosphere–Ocean Climate System*, edited by W. K. M. Lau and D. E. Waliser, pp. 19–61, Springer, Berlin, doi:10.1007/3-540-27250-X 2.
- Goswami, B. N. (2005b), The Asian monsoon: Interdecadal variability, in *The Asian Monsoon*, edited by B. Wang, pp. 295–327, Springer, New York.
- Goswami, B. N., and P. K. Xavier (2005a), Dynamics of “internal” interannual variability of Indian summer monsoon in a GCM, *J. Geophys. Res.*, *110*, D24104, doi:10.1029/2005JD006042.
- Goswami, B. N., and P. K. Xavier (2005b), ENSO control on the South Asian monsoon through the length of the rainy season, *Geophys. Res. Lett.*, *32*, L18717, doi:10.1029/2005GL023216.
- Goswami, B. N., V. Krishnamurthy, and H. Annamalai (1999), A broad-scale circulation index for interannual variability of the Indian summer monsoon, *Q. J. R. Meteorol. Soc.*, *125*, 611–633, doi:10.1002/qj.49712555412.
- Goswami, B. N., G. Wu, and T. Yasunari (2006), The annual cycle, intraseasonal oscillations, and roadblock to seasonal predictability of the Asian summer monsoon, *J. Clim.*, *19*, 5078–5099, doi:10.1175/JCLI3901.1.
- Hayashi, Y. (1980), Estimation of nonlinear energy transfer spectra by the cross-spectral method, *J. Atmos. Sci.*, *37*, 299–307, doi:10.1175/1520-0469(1980)037<0299:EONETS>2.0.CO;2.
- Hayashi, Y.-Y., and A. Sumi (1986), The 20–30-day oscillations simulated in an “aqua planet” model, *J. Meteorol. Soc. Jpn.*, *64*, 451–467.
- Hendon, H. H., and M. L. Salby (1994), The life cycle of the Madden-Julian Oscillation, *J. Atmos. Sci.*, *51*, 2225–2237, doi:10.1175/1520-0469(1994)051<2225:TLCOTM>2.0.CO;2.
- Hoskins, B. J., and B. Wang (2005), Large-scale atmospheric dynamics, in *The Asian Monsoon*, edited by B. Wang, chap. 9, pp. 357–415, Springer, New York.
- Hoyos, C. D., and P. J. Webster (2007), The role of intraseasonal variability in the nature of Asian monsoon precipitation, *J. Clim.*, *20*, 4402–4424, doi:10.1175/JCLI4252.1.
- Joseph, S., A. K. Sahai, and B. N. Goswami (2009), Eastward propagating MJO during boreal summer and Indian monsoon droughts, *Clim. Dyn.*, *32*, 1139–1153, doi:10.1007/s00382-008-0412-8.
- Kalnay, E., et al. (1996), The NCEP/NCAR 40-Year Reanalysis Project, *Bull. Am. Meteorol. Soc.*, *77*, 437–471, doi:10.1175/1520-0477(1996)077<0437:TNYRP>2.0.CO;2.
- Kemball-Cook, S., and B. Wang (2001), Equatorial waves and air–sea interaction in the boreal summer intraseasonal oscillation, *J. Clim.*, *14*, 2923–2942, doi:10.1175/1520-0442(2001)014<2923:EWAASI>2.0.CO;2.
- Kiladis, G. N., M. C. Wheeler, P. T. Haertel, K. H. Straub, and P. E. Roundy (2009), Convectively coupled equatorial waves, *Rev. Geophys.*, *47*, RG2003, doi:10.1029/2008RG000266.
- Krishnamurthy, V., and B. N. Goswami (2000), Indian monsoon–ENSO relationship on interdecadal timescale, *J. Clim.*, *13*, 579–595, doi:10.1175/1520-0442(2000)013<0579:IMEROI>2.0.CO;2.
- Krishnamurti, T. N., A. Thomas, A. Simon, and V. Kumar (2010), Desert air incursions, an overlooked aspect, for the dry spells of Indian summer monsoon, *J. Atmos. Sci.*, *67*, 3423–3441, doi:10.1175/2010JAS3440.1.
- Krishnan, R., V. Kumar, M. Sugi, and J. Yoshimura (2009), Internal feedbacks from monsoon–midlatitude interactions during droughts in the

- Indian summer monsoon, *J. Atmos. Sci.*, *66*, 553–578, doi:10.1175/2008JAS2723.1.
- Kumar, K. K., B. Rajagopalan, and M. A. Cane (1999), On the weakening relationship between the Indian monsoon and ENSO, *Science*, *284*, 2156–2159, doi:10.1126/science.284.5423.2156.
- Madden, R. A., and P. R. Julian (1972), Description of global-scale circulation cells in the tropics with a 40–50 day period, *J. Atmos. Sci.*, *29*, 1109–1123, doi:10.1175/1520-0469(1972)029<1109:DOGSCC>2.0.CO;2.
- Madden, R. A., and P. R. Julian (1994), Observations of the 40–50 day tropical oscillation—A review, *Mon. Weather Rev.*, *122*, 814–837, doi:10.1175/1520-0493(1994)122<0814:OOTDIO>2.0.CO;2.
- Maloney, E. D., and D. L. Hartmann (2001), The Madden-Julian Oscillation, barotropic dynamics, and North Pacific tropical cyclone formation. Part I: Observations, *J. Atmos. Sci.*, *58*, 2545–2558, doi:10.1175/1520-0469(2001)058<2545:TMOJBD>2.0.CO;2.
- Masanaga, H. (2007), Seasonality and regionality of the Madden-Julian Oscillation, Kelvin wave, and equatorial Rossby wave, *J. Atmos. Sci.*, *64*, 4400–4416, doi:10.1175/2007JAS2179.1.
- Matsuno, T. (1966), Quasi-geostrophic motions in the equatorial area, *J. Meteorol. Soc. Jpn.*, *44*, 25–43.
- Neena, J. M., and B. N. Goswami (2010), Extension of potential predictability of Indian summer monsoon dry and wet spells in recent decades, *Q. J. R. Meteorol. Soc.*, *136*, 583–592.
- Paï, D. S., J. Bhate, O. P. Sreejith, and H. R. Hatwar (2009), Impact of MJO on the intraseasonal variation of summer monsoon rainfall over India, *Clim. Dyn.*, *36*, 41–55, doi:10.1007/s00382-009-0634-4.
- Ramaswamy, C. (1962), Breaks in the Indian summer monsoon as a phenomenon of interaction between easterly and the subtropical westerly jet streams, *Tellus*, *14*, 337–349, doi:10.1111/j.2153-3490.1962.tb01346.x.
- Ratnam, J. V., S. K. Behera, Y. Masumoto, K. Takahashi, and T. Yamagata (2010), Pacific Ocean origin for the 2009 Indian summer monsoon failure, *Geophys. Res. Lett.*, *37*, L07807, doi:10.1029/2010GL042798.
- Roundy, P. E., and W. M. Frank (2004), Effects of low-frequency wave interactions on intraseasonal oscillations, *J. Atmos. Sci.*, *61*, 3025–3040, doi:10.1175/JAS-3348.1.
- Roundy, P. E., C. J. Schreck, and M. A. Janiga (2009), Contributions of convectively coupled equatorial Rossby waves and Kelvin waves to the real-time multivariate MJO indices, *Mon. Weather Rev.*, *137*, 469–478, doi:10.1175/2008MWR2595.1.
- Sikka, D., and S. Gadgil (1980), On the maximum cloud zone and the ITCZ over Indian, longitudes during the southwest monsoon, *Mon. Weather Rev.*, *108*, 1840–1853, doi:10.1175/1520-0493(1980)108<1840:OTMCZA>2.0.CO;2.
- Sikka, D. R., A. Tyagi, and L. C. Ram (2010), Large scale fluctuations of the continental tropical convergence zone (CTCZ) during pilot CTCZ phase-2009 and the evolution of monsoon drought in 2009, *Mausam*, *61*(1), 47–74.
- Suhas, E., and B. N. Goswami (2008), Regime shift in Indian summer monsoon climatological intraseasonal oscillations, *Geophys. Res. Lett.*, *35*, L20703, doi:10.1029/2008GL035511.
- Wang, B., and Z. Fan (1999), Choice of South Asian summer monsoon indices, *Bull. Am. Meteorol. Soc.*, *80*, 629–638, doi:10.1175/1520-0477(1999)080<0629:COSASM>2.0.CO;2.
- Wang, B., and X. Xie (1997), A model for the boreal summer intraseasonal oscillation, *J. Atmos. Sci.*, *54*, 72–86, doi:10.1175/1520-0469(1997)054<0072:AMFTBS>2.0.CO;2.
- Webster, P. J. (1987), The variable and interactive monsoon, in *Monsoons*, edited by J. S. Fein and P. L. Stephens, pp. 269–330, John Wiley, Hoboken, N. J.
- Wheeler, M. C., and H. H. Hendon (2004), An all-season real-time multivariate MJO index: Development of an index for monitoring and prediction, *Mon. Weather Rev.*, *132*, 1917–1932, doi:10.1175/1520-0493(2004)132<1917:AARMMI>2.0.CO;2.
- Wheeler, M., and G. N. Kiladis (1999), Convectively coupled equatorial waves: Analysis of clouds and temperature in the wavenumber-frequency domain, *J. Atmos. Sci.*, *56*, 374–399, doi:10.1175/1520-0469(1999)056<0374:CCEWAO>2.0.CO;2.
- Wheeler, M. C., H. Hendon, S. Cleland, H. Meinke, and A. Donald (2009), Impacts of the Madden-Julian Oscillation on Australian rainfall and circulation, *J. Clim.*, *22*, 1482–1498, doi:10.1175/2008JCLI2595.1.
- Xavier, P. K., C. Marzin, and B. N. Goswami (2007), An objective definition of the Indian summer monsoon season and a new perspective on ENSO-monsoon relationship, *Q. J. R. Meteorol. Soc.*, *133*, 749–764, doi:10.1002/qj.45.

B. N. Goswami, J. M. Neena, and E. Suhas, Indian Institute of Tropical Meteorology, Dr. Homi Bhabha Road, Pashan, Pune, Maharashtra 411008, India. (goswami@tropmet.res.in)